Importance of Plasticity for GISSMO Calibration in Automotive Safety Applications

Dr. Richard Burrows

NIO Performance Engineering, Oxford, UK

1 Introduction

GISSMO has become an incredibly flexible tool since its inception. An overview is not to be presented here owing to the fact it is coved extensively by other authors. This body of work aims to show that even using simple techniques and features a robust GISSMO card is possible using only **`*MAT_024`** and **`*MAT_ADD_EROSION`**, that can be useful in automotive safety, even with larger type 16 shell elements 3-6mm in edge length for gauges approx. 1-2mm. 3-6mm quad elements are a very useful size for automotive structures and allows accurate meshing of holes, flanges and joints for example.

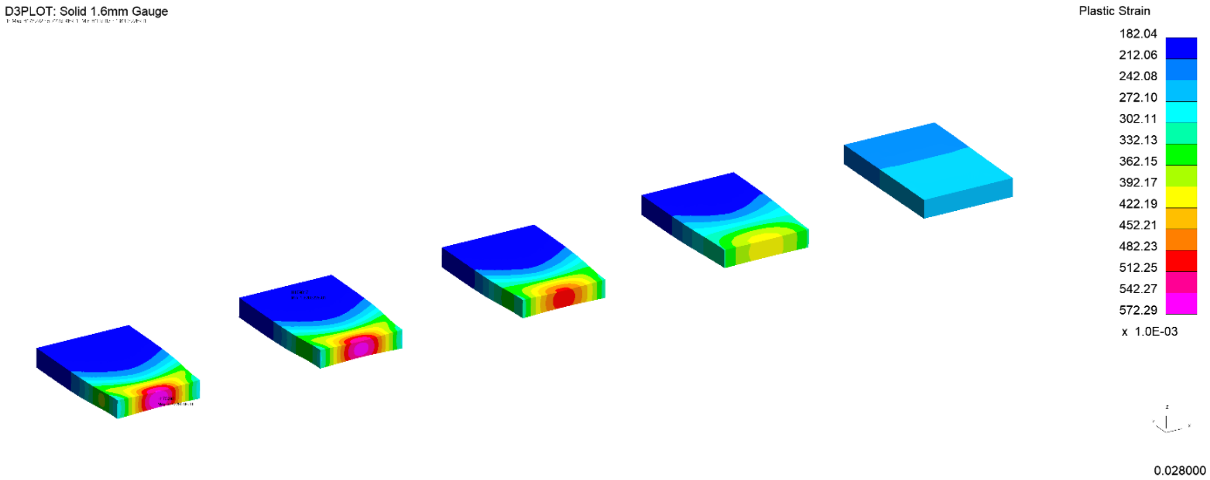

Fig.1: Plastic Strain of 6mm x 6mm x 1.6mm squares, the size to which a GISSMO failure card is constructed in this work. Displacement applied would give 25% engineering strain

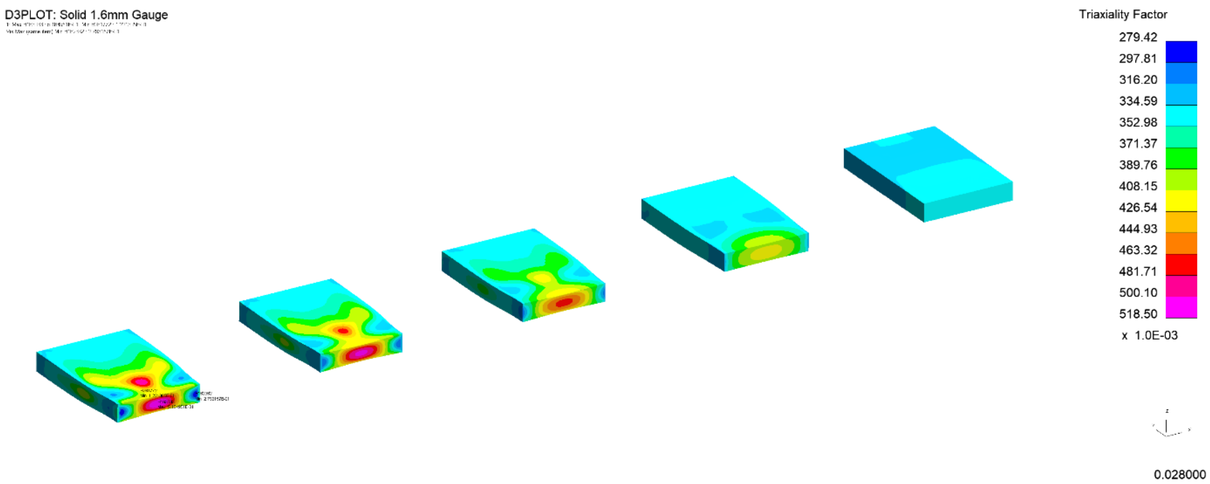

Fig.2: Triaxiality of 6mm x 6mm x 1.6mm squares, the size to which a GISSMO failure card is constructed in this work. 20-15-10-5-2 elements through thickness left to right. Boundary conditions to give uniaxial tension loading

Fig 1 and fig 2 set the scene of what we are trying to model in automotive BIW crash CAE: the necking which always precedes failure for ductile metals. Solid elements allow CAE to capture the necking process however much more typical is to model BIW with larger shell elements. The author proposes using the larger shells, useful for CAE simulations due to their speed of solution for high frequency iterations in automotive product development cycles, but also because they can avoid modelling of the through thickness neck seen typically before failure of metallic sheet materials. One can crudely describe a neck to be around the gauge of ductile sheet materials; and by using elements significantly larger than this we simplify our model and aim not on perfect geometrical discretisation, but for an element that aims to mimic the behaviour of the neck within. This has important consequences for the engineering decisions around specifying a flow curve.

2 Testing – Flow Curve Determination

We describe here the data necessary for a useful GISSMO card for DP600, DP800 and PHS2000 grades of steel. We will walk through the testing package starting with plasticity before moving onto fracture.

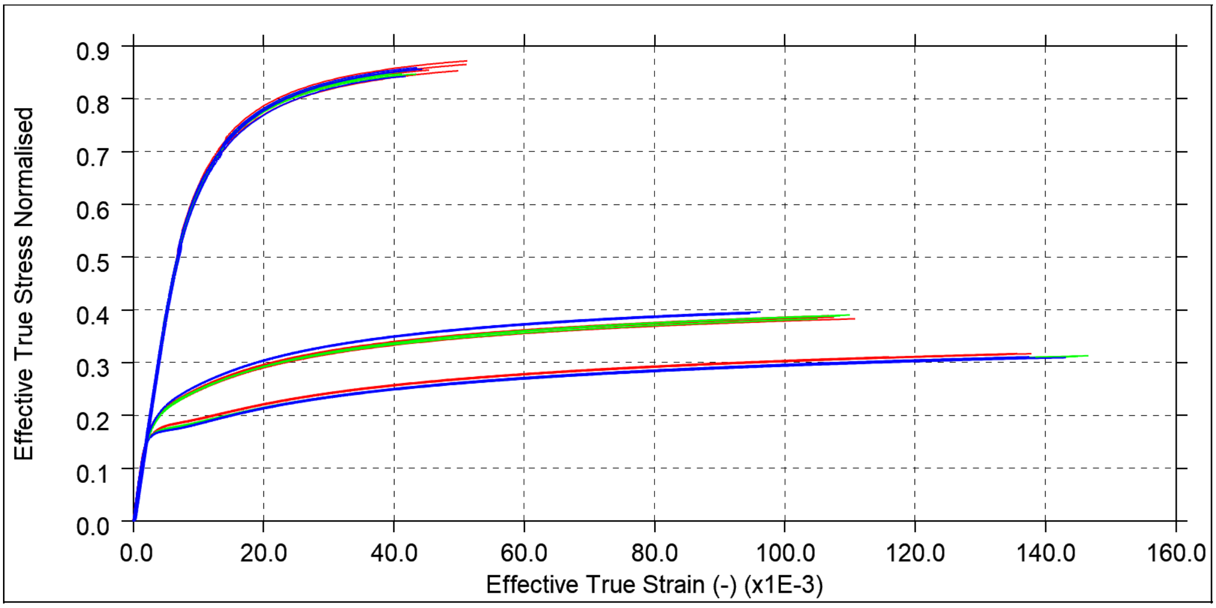

Fig.3: Uniaxial tension tests. Red (rolling direction) green (diagonal direction) and blue (transverse direction)

Fig 3 shows that isotropic behaviour can be used for the constitutive model. Though maybe not for stamping simulations, isotropic behaviour can be assumed here for the purpose of crash CAE. Below in fig 4 the addition of hydraulic bulge tests provides work hardening information to much higher strain levels than uniaxial tension tests due to the fact that there is no necking process observed in this test.

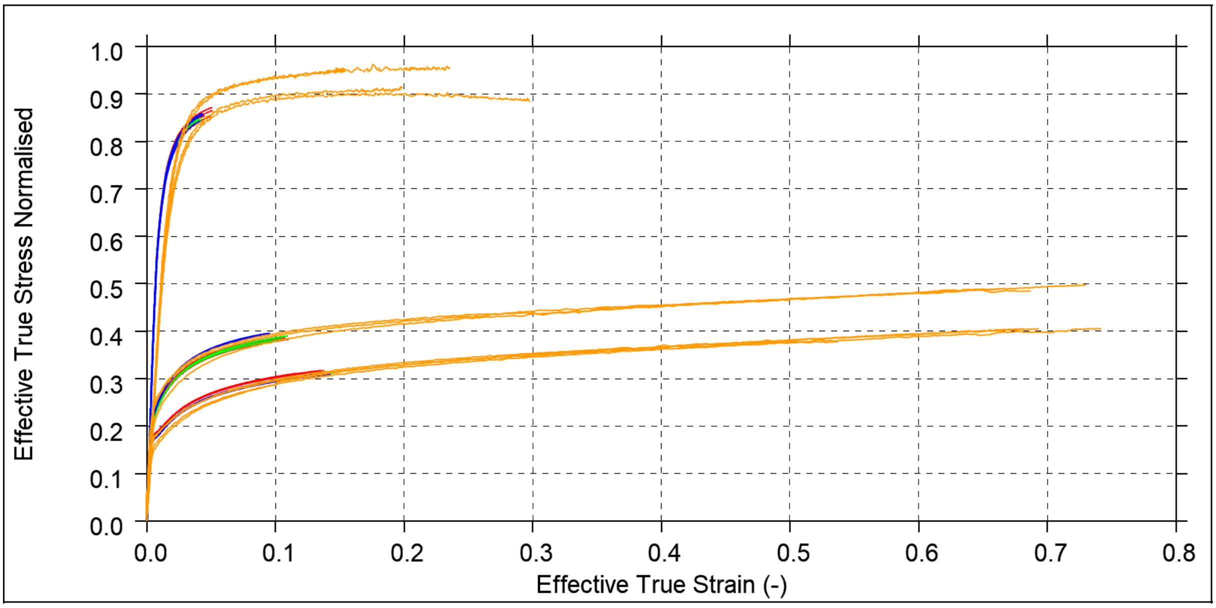

Fig.4: Uniaxial tension tests from fig 3 with addition of hydraulic bulge test results shown in orange

3 Testing – Fracture Locus Determination

To capture the failure strains Digital Image Correlation (DIC) is used for several geometries. Reverse engineering can be done to create a GISSMO fracture model but with DIC one has concrete information and a good place to start. Care has to be taken to avoid fracture initiation from sample edges at all times and can be challenging.

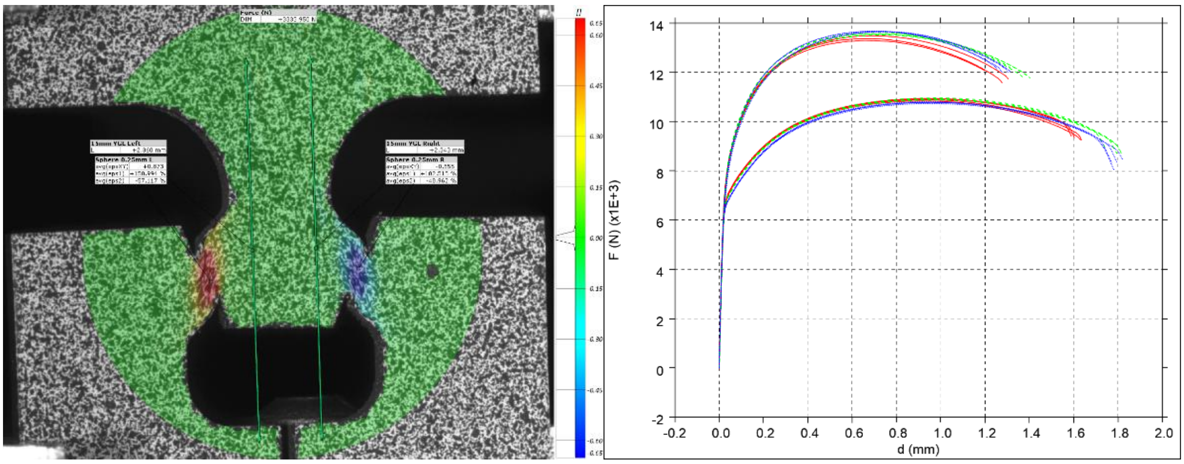

Fig.5: Shear coupon tested with DIC. Red (rolling direction) green (diagonal direction) and blue (transverse direction)

Double ligand shear tests as shown in fig 5 offer a good opportunity to measure failure strain at very close to zero triaxiality. Careful design of the ligands with a slight offset prevents fracture in uniaxial tension because during the shear deformation the lateral compression keeps the shear mode dominant. Not only this but additionally the overall appreciation of the plastic shearing process can be seen from the F-d plot. We see again that isotropic behaviour is present. No effort here is made for a 45° shear sample because the loading is not proportional.

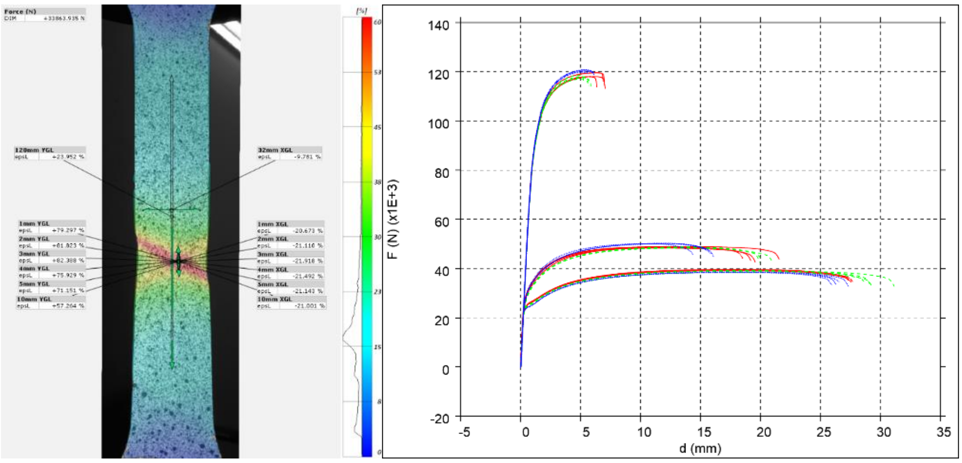

Fig.6: Uniaxial tension of a large 40mm wide geometry ASTM A200. Red (rolling direction) green (diagonal direction) and blue (transverse direction)

In fig 6 above one can again see that there is little appreciable anisotropy, though more noticeable than all other tests described above and below. DP800 has the most significant anisotropy though is still taken here as negligible. The 40mm wide sample allows for CAE to be performed as part of the verification process.

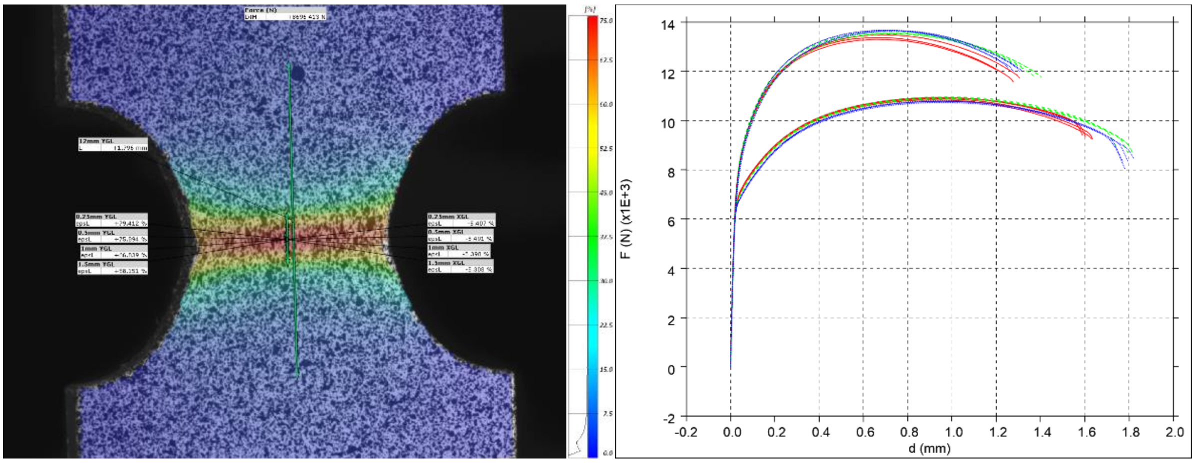

Fig.7: Plane strain tension. No test was performed on PHS2000. Red (rolling direction) green (diagonal direction) and blue (transverse direction)

Plane strain VDA bending is also another route to getting failure strains and is depicted below. DIC is also performed but it is not so obvious to the reader what it is as a close up image but important is the small zone of plastic deformation and failure. Bending for type 16 shells is very difficult to perform in CAE. It is quite critical in thicker parts of the BIW but with ductile thin metals we at least see few failures in this mode, thus it can be conveniently ignored. Even calculating the effective strain to failure is difficult because metals bend at such tight radii as in this work no longer obey Vermicelli theory. We do again observe isotropic behaviour though in fig 8 below.

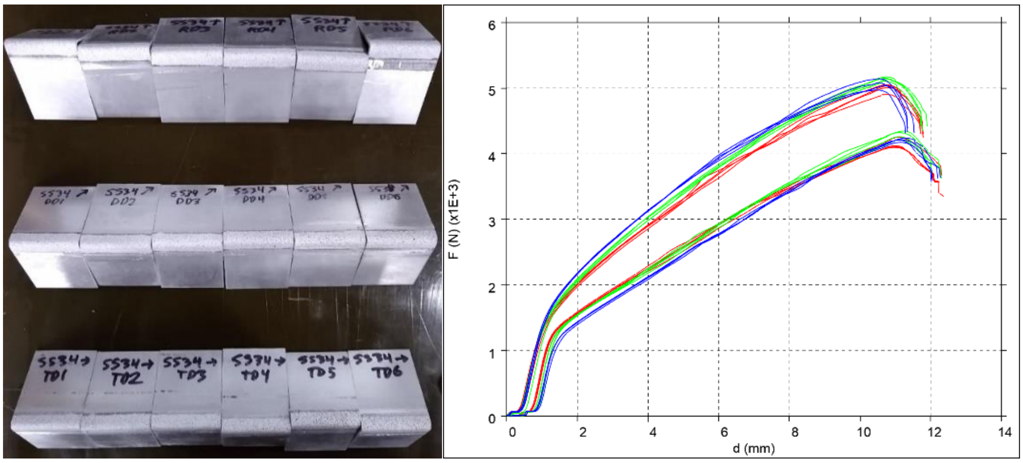

Fig.8: VDA bending test. Red (rolling direction) green (diagonal direction) and blue (transverse direction)

A final option explored in this work for measuring plane strain failure is using Marciniak FLC samples to not measure necking, but fracture. It has the distinct advantage because one has a larger area in plane strain than with the 8-10mm in a coupon.

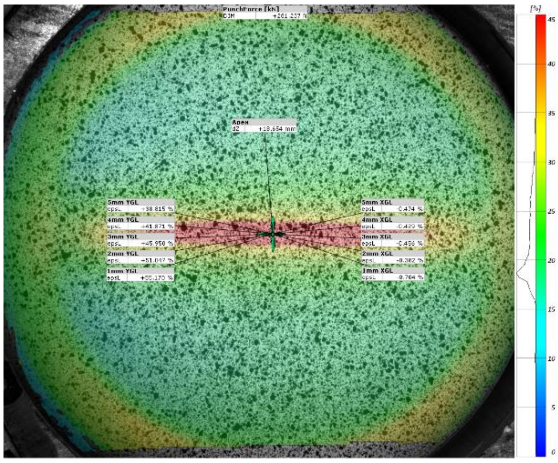

Fig.9: DIC image taken from above a Marciniak punch sample in plane strain

A Nakajima punch with a full sample is an easy test for getting failure strains over a large area. Even using artificial strain gauges above 10mm we observe the same failure strain when using the last image before failure.

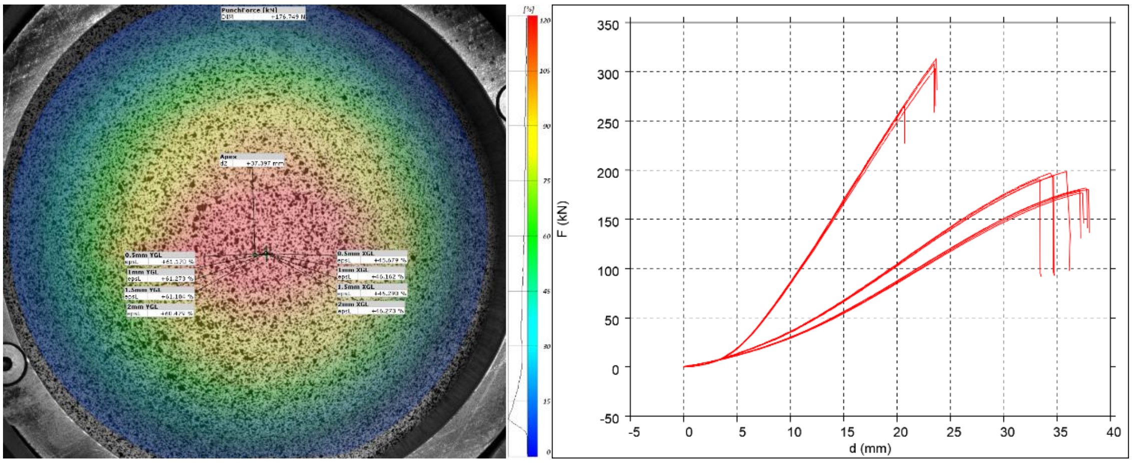

Fig.10: Nakajima biaxial punch test. Of course only one direction can be assumed with ease however.

Above the author describes only the overall plastic response up to failure using the F-d plots. The benefit of DIC data is that it captures 3D strain information and can be interrogated to get failure strains. It can be taken as an area average – which is used in this work only for the shear test – or by specifying artificial strain gauges. The software can be used extract strain information for many artificial strain ague lengths and area averages and the author suggests using these close to the element sizes intended for the calibration.

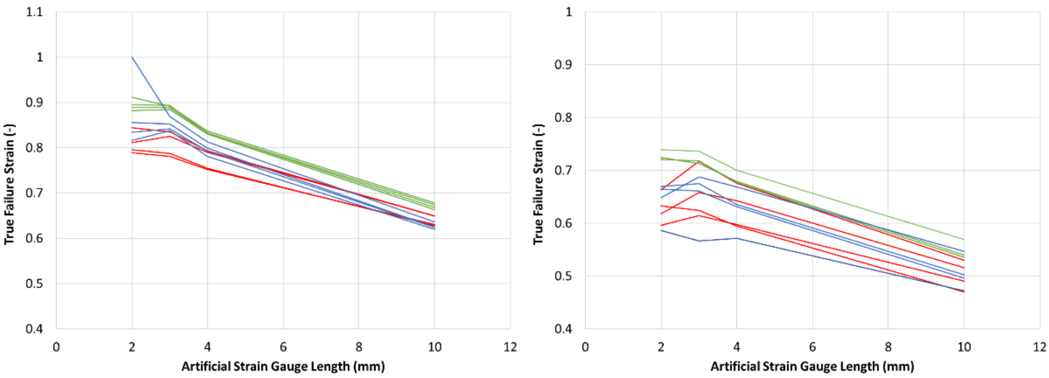

Uniaxial failure at 2-3-4-10mm artificial strain gauge lengths for (a) DP600 and (b) DP800

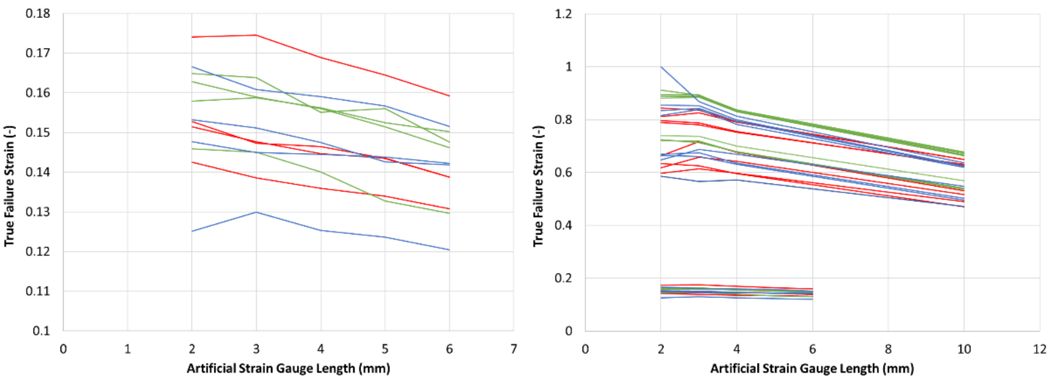

Fig.11: Uniaxial failure at 2-3-4-10mm artificial strain gauge lengths for (c) PHS2000 and (d) then all together on one graph. Red (rolling direction) green (diagonal direction) and blue (transverse direction). Scaled to give a max strain of 1.0 over all failure strains seen in this document

From the uniaxial test results above in fig 11; looking closer at the failure strains, rather than the macro plastic F-d curve, there is slightly more observable anisotropy. Also noteworthy is it doesn't appear consistent for all grades tested here that the transverse direction is the least formable, as is traditionally measured on steels for FLCs and specifying minimum quality targets.

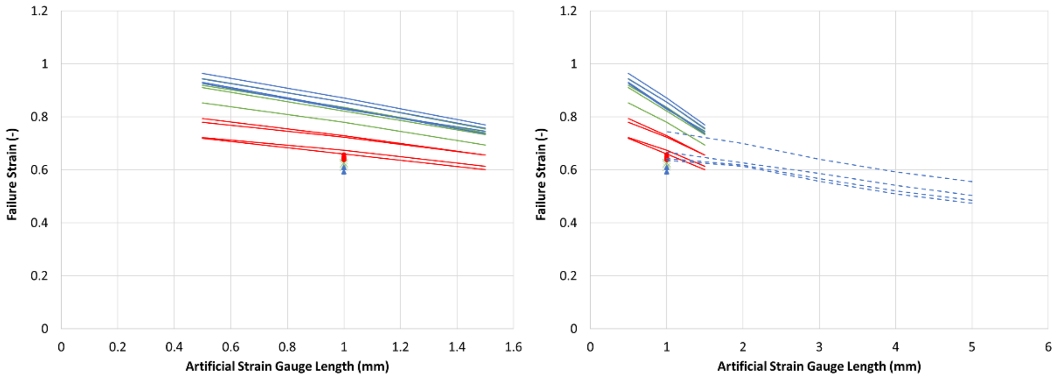

Plane strain failure strains for DP600 (a) just with bending results and plane strain tension samples then (b) with the addition of Marciniak samples.

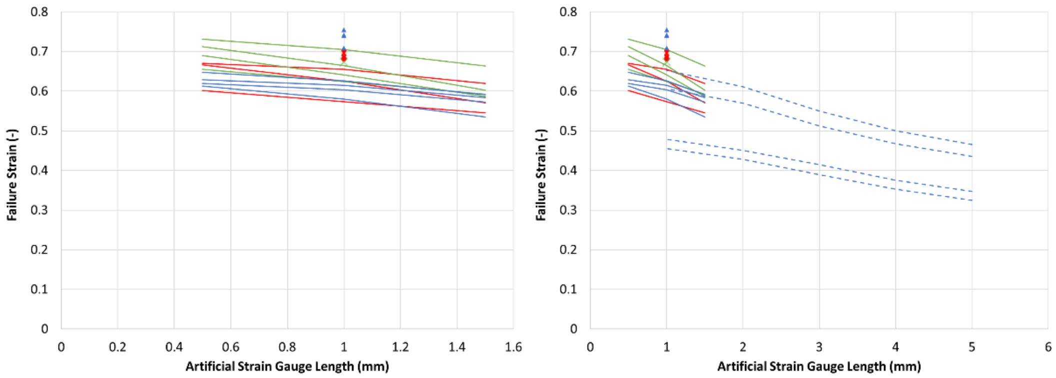

Fig.12: Plane strain failure strains for DP800 (c) just with bending results and plane strain tension samples then (d) with the addition of Marciniak samples.

Owing to the fact that the author was experimenting with different techniques to define plane strain failure for the DP grades, there are three test results to discuss. The advantage is clearly seen in fig 12 for the Marciniak measured results because they can be argued as valid at larger artificial strain gauge lengths.

4 Testing – High Strain Rate Behaviour

Few areas of formability and fracture testing are as challenging as high speed tension testing but modern hydraulic load frames and high speed cameras mean this can be much more readily achieved than a decade or two ago. A point to remember when performing tests over multiple strain rates is to use the same coupon geometry because there is a shape factor whereby smaller sample see larger engineering strains to failure and higher strain rates in the neck. The scale factor in fig 13 one can see is of UTS and the results are difficult to use in a similar way for failure strain so this is not shown or used in this work.

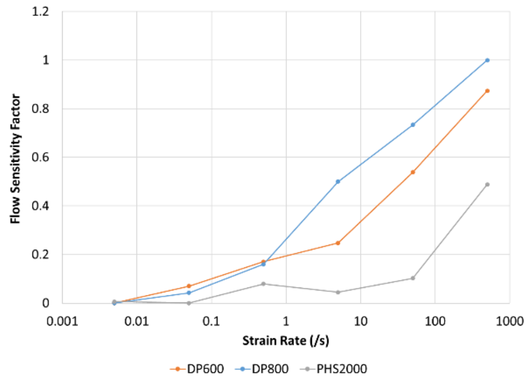

Fig.13: High strain rate tension tests performed on a hydraulic tension frame and high speed DIC. Results displayed as a UTS sensitivity factor with 1 being the full sensitivity of DP800 at 500/s

5 GISSMO Card Creation

As stated in the introduction, a **`*MAT_024`** card with **`*MAT_ADD_EROSION`** is the target of this work to be used in automotive safety applications with shell elements 3-6mm and be as simple as possible. Pertinent values for the reader would be both damage exponent and stress fadeout exponent equal to 2, b SHRF and BIAXF equal to -1 and DMGTYP equal to 1.

In light of the data shown in figs 3-12 the author is recommending isotropic behaviour be assumed for crash applications. The flow curve is taken from quasi-static uniaxial tension tests with an average value for the relevant material: in this worked example DP800. Extrapolation using a modified voce equation that is forced to saturation by setting K=1 in equation 1 below:

$$\sigma_Y = B + \left(A + K\varepsilon_p\right)\left[1 - e^{-\frac{C}{A}\varepsilon_p}\right]$$

With A being hardening, B the onset of plasticity and c a shape coefficient. Coefficients over the final 1% of uniform plastic deformation are recommended for the fitting. This gives different flow behaviour to what we measure in hydraulic bulge testing, however casting our mind back to figs 1 & 2 remember we are aiming to model the necking process with shells that are much larger than a neck geometry.

The above approach seems to correlate well to CAE and the importance of flow stress to the overall calibration cannot be stressed enough, with the damage model determining the softening process post localisation. To put it another way, using the hydraulic bulge test data for flow curve creation one would require a much different GISSMO calibration.

For shear and lower triaxiality the area average from inside the shear ligand can be used as a simple average between all results. Similarly this approach is recommended to be used for the biaxial failure points. For the uniaxial tension and plane strain failure points the failure strains can be taken from approximately 6mm artificial strain gauge lengths. Joining them all up with simple power 2 parabolas creates the familiar W shape seen below in fig14. Additionally, the true strain at UTS in uniaxial tension is used for the bottom of the localisation parabola, which is using a power 5 function to then finish a token amount of strain higher than the shear and biaxial failure strains. With shrf and biaxf being set to -1 this ensures regularisation between the intersections of the below two curves.

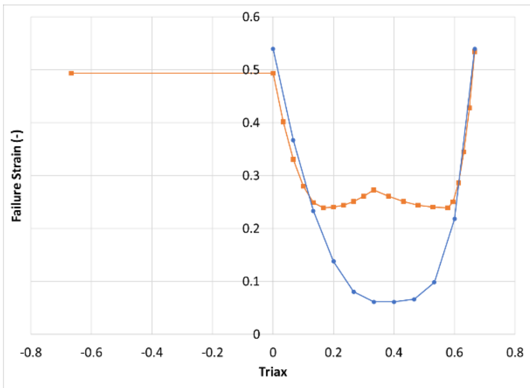

Fig.14: Failure and localisation curves for DP800. Power 2 parabolas used to describe the failure curve and power 5 parabolas used to describe the localisation curve. Scaled by same factor as fig 11

Shear and biaxial tension failure is not the most predominant mode of failure in sheet metal stamped parts in the body in white, the target application of this calibration, however it is interesting for the reader to note that neither are mesh size dependent. Shear deformation does not localise, even if we did see lots of shear deformation the thin sheet part will buckle. Biaxial we have measured from 1mm to above 10mm artificial strain gauge lengths giving identical failure strains and the size of high strain is clearly seen in fig 10.

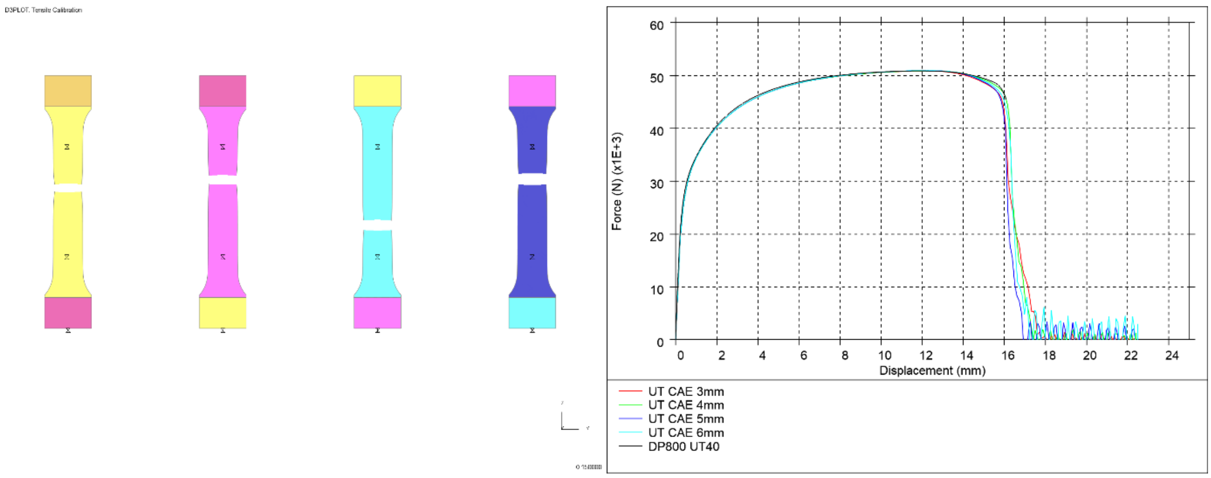

Fig.15: Result of the simple tuning process on a large ASTM A200 (40mm wide) sample

Fig 15 above is the result of the simple tuning process on DP800. No other parameters are changed other than the regularisation curve which increases failure strains above 1 at for elements less than 6mm using a simple parabola. This is why we used a 6mm artificial strain gauge length from the raw data and focused, where possible, for large samples to enable this. Following the simple calibration process the flow curve is replaced with a table describing the flow behaviour between 0.005 and 500 /s and the card is ready to use. It is worth noting that the shear band seen in fig 6 is not replicated in fig 15 and this is, as far as the author can say, a limitation of larger elements.

For use in full vehicle CAE there are some recommendable steps to take into account the most important manufacturing processes which appreciably change the mechanical behaviour of sheet materials. Firstly the mapping of the forming strains and thinning is crucial. As typical auto body panels won't have been formed beyond the start of localisation, mapping of damage variables can more than likely be omitted. The next most important to consider would be for steels, especially DP steels stronger than 800MPa, would be the Heat Affected Zone around spot welds. Above 1000MPa the amount of martensite in the grades gets significantly tempered by the heat of the welding process causing a significant strength reduction. A scaled GISSMO card can help. Finally, important not to forget some steels have a significantly reduced ductility in sheared edges. For DP600, a very significant sensitivity is witnessed and ductility drops even below the strain at UTS. A tuned simple `*MAT_024` card can model this quite sufficiently, as no necking means no mesh sensitivity and no GISSMO being required. This is interesting to consider due to the fact that sensitive edges are a regular fracture initiation point, but their behaviour being brittle means that they can be given a simple treatment.

6 Summary

A simple approach has been presented to make a GISSMO card with minimal tuning in the hope of staying close to reality and making an accurate CAE card for type 16 shell elements 3-6mm in edge length. The data for three important steel grades is presented and the methodology for translating this to a GISSMO card is given step by step for DP800. Some additional recommended steps are also briefly described to allow accurate industrial use.

Assigning yield and flow properties for GISSMO cards can be a challenge. Materials such as common steel grades used for safety relevant automotive structures are observed as being comparatively isotropic. The flow behaviour does however seem to be quite challenging to define and the author suggests this is because flow curve and the damage parameters of the GISSMO *tune* means it is difficult to separate and thus conclude what effect we are observing. Higher work hardening forces us to use lower fracture locus and parameters to cause more softening to be able to repeat the humble tension test in CAE.

Further investigation is required on the plane strain tension samples to give a F-d curve to validate against, whilst also giving failure in the centre of the sample comparable to that seen in the Marciniak test. Loading for different coupon geometries is an important part of verification or tuning. VDA bending results are important for determining a bending factor for more sophisticated GISSMO cards not covered here. It is not yet conclusive if one plane strain test should be favoured over the other. More brittle metals and thicker sections will give lots of failure in bending for example so require a different process as outlined and recommended here.